Quantitative Scaling of Magnetic Avalanches

G. Durin,[1,2] F. Bohn,[3] M. A. Corrêa,[3] R. L. Sommer,[4] P. Le Doussal,[5] and K. J. Wiese[5]

[1]*Istituto Nazionale di Ricerca Metrologica, Strada delle Cacce 91, 10135 Torino, Italy*
[2]*ISI Foundation, Via Alassio 11/c, 10126 Torino, Italy*
[3]*Departamento de Física Teórica e Experimental, Universidade Federal do Rio Grande do Norte, 59078-900 Natal, RN, Brazil*
[4]*Centro Brasileiro de Pesquisas Físicas, Rua Dr. Xavier Sigaud 150, Urca, 22290-180 Rio de Janeiro, RJ, Brazil*
[5]*CNRS-Laboratoire de Physique Théorique de l'Ecole Normale Supérieure, 24 rue Lhomond, 75005 Paris, France*

We provide the first quantitative comparison between Barkhausen noise experiments and recent predictions from the theory of avalanches for pinned interfaces, both in and beyond mean field. We study different classes of soft magnetic materials, including polycrystals and amorphous samples—which are characterized by long-range and short-range elasticity, respectively—both for thick and thin samples, i.e., with and without eddy currents. The temporal avalanche shape at fixed size as well as observables related to the joint distribution of sizes and durations are analyzed in detail. Both long-range and short-range samples with no eddy currents are fitted extremely well by the theoretical predictions. In particular, the short-range samples provide the first reliable test of the theory beyond mean field. The thick samples show systematic deviations from the scaling theory, providing unambiguous signatures for the presence of eddy currents.

Barkhausen noise in soft magnets originates from the jerky motion of magnetic domain walls (DWs), and is characterized by scale-free power-law distributions of magnetization jumps [1–6]. It is the earliest and most scrutinized probe for avalanche motion, an ubiquitous phenomenon present in systems such as fluid contact-line depinning [7,8], brittle fracture fronts [9,10], and pinned vortex lines [11]. In all these systems the motion of an overdamped elastic interface (of internal dimension d) driven in a quenched medium was proposed as an efficient mesoscopic description. However, until now, analytical predictions allowing for a detailed comparison with experiments have been scarce, due to the difficulty in treating collective discontinuous jumps in presence of many metastable states.

Toy models have thus been developed, capturing essential features at the level of mean field (MF). One celebrated example is the ABBM model, where the domain wall is modeled as a single point in an "effective" random force landscape performing a (biased) Brownian motion [12–14]. Refinements based on infinite-range models were later proposed [15], leading to similar physics [14,16]. These MF toy models predict an avalanche-size distribution $P(S) \sim S^{-\tau}$ with $\tau = \tau_{\mathrm{MF}} = 3/2$ and a duration distribution $P(T) \sim T^{-\alpha}$ with $\alpha = \alpha_{\mathrm{MF}} = 2$.

The theory of interface depinning provides a predictive universal framework for the avalanche statistics. It involves two independent exponents, the roughness exponent ζ and the dynamical exponent z. The distribution exponents α and τ were conjectured from scaling, as in the Narayan-Fisher (NF) conjecture $\tau = 2 - \mu/(d + \zeta)$ and $\alpha = 1 + (d + \zeta - \mu)/z$, where μ describes the range of interactions.

The upper-critical dimension at which $\zeta = 0$ and below which mean-field models fail is $d_{\mathrm{uc}} = 4$ for short-range elasticity (SR, $\mu = 2$) and $d_{\mathrm{uc}} = 2$ for long-range elasticity (LR, $\mu = 1$) [16].

In Barkhausen noise experiments, two distinct families of samples were identified, consistent with these predictions [17]. In polycrystalline materials, the DW experiences strong anisotropic crystal fields leading to LR elasticity. In the $D = d + 1 = 2 + 1$ geometry this system behaves according to MF theory. In amorphous samples, SR elasticity prevails over a negligible LR elasticity, and the avalanche exponents agree with the NF prediction. In both cases, a relevant role is played by the demagnetizing field, which acts as a cutoff for large avalanches [17]. These mean-field predictions were tested in soft magnetic thin films, where the retarding effects of eddy currents (ECs) of bulk samples are negligible [6].

Recently, it became possible to compare theory and experiments of avalanches well beyond scaling and the value of exponents. On the theoretical side, the functional renormalization group of depinning was extended to calculate a host of avalanche observables [18–23]. Examples are the avalanche shape at fixed size and duration as well as the joint size distribution both in mean field and beyond, even including retardation effects due to eddy currents [24]. On the experimental side, the avalanche shape was studied in magnetic systems [6,25], in fracture and imbibition [26]. Despite these experiments, most of the recent predictions of the theory have not yet been tested quantitatively, and especially not to high accuracy.

The aim of this Letter is to provide new and sensitive tests of these theoretical predictions in soft ferromagnets.

This is possible because we detected in our Barkhausen experiment a high number of avalanches, obtaining a robust statistics. Diverse magnetic samples have been explored, corresponding to the two universality classes (LR and SR), with and without EC effects. We focus our attention on the avalanche shape at fixed size and observables linked to the joint distribution of sizes and durations. The SR and LR samples with no ECs fit extremely well with the theoretical predictions. In particular, the SR samples for the first time provide a significant test of the theory beyond mean field. The effect of eddy currents on the scaling properties is also investigated.

We start by presenting the predictions from the theory of elastic interfaces that we aim to test [20–23]. These predictions are calculated for avalanches following an infinitesimal increase in the field (kick). They also apply to the stationary, quasistatic regime in the limit of slow driving, as performed in experiments [22]. The interface model involves a (small) mass m^2, which flattens the interface beyond the scale $1/m$, playing the same role as the demagnetizing field in setting the cutoff scale. Associated to the two independent exponents ζ and z are two independent scales $S_m \simeq m^{-d+\zeta}$ and $\tau_m \simeq m^{-z}$ for sizes and durations. The size scale S_m can be directly measured in the experiments as

$$S_m = \frac{\langle S^2 \rangle}{2\langle S \rangle}, \tag{1}$$

where $\langle \dots \rangle$ denotes expectation values with respect to $P(S)$. On the other hand, the time scale τ_m cannot be determined analytically, and has to be guessed from data, as we explain later. We denote by $u(x,t)$ the displacement field of the interface, $x \in \mathbb{R}^d$, and by $\dot{u}(t) = \int d^d x \, \dot{u}(x,t)$ the time derivative of the total swept area. The avalanche size is $S = \int_0^T dt \, \dot{u}(t)$.

The simplest observables we can consider are the moments of the average size at fixed duration

$$\langle S^n \rangle_T = (S_m)^n g_n(T/\tau_m), \qquad g_n(\tilde{T}) \simeq_{\tilde{T} \to 0} c_n \tilde{T}^{n\gamma}, \tag{2}$$

whose universal behavior for small avalanches defines the exponent γ. Here, $\tilde{T} = T/\tau_m$ is the rescaled avalanche duration. In mean field, one finds

$$\gamma^{MF} = 2, \qquad c_1^{MF} = \frac{1}{3}, \qquad c_2^{MF} = \frac{2}{15}, \tag{3}$$

and the scaling functions are

$$g_1^{MF}(\tilde{T}) = 2\tilde{T} \coth(\tilde{T}/2) - 4,$$

$$g_2^{MF}(\tilde{T}) = 2\tilde{T} \operatorname{csch}^2\left(\frac{\tilde{T}}{2}\right)\{\tilde{T}[\cosh(\tilde{T}) + 2] - 3\sinh(\tilde{T})\}. \tag{4}$$

Beyond mean field, one finds

$$\gamma = \frac{d + \zeta}{z}, \qquad c_1 = c_1^{MF} + \frac{11 - 3\gamma_E - \ln 4}{81}\epsilon, \tag{5}$$

where the expression for c_1 has been calculated to first order in $\epsilon = d_{uc} - d$. This leads to $c_1 \approx 0.527$ for $\epsilon = 2$, as in the case of $\mu = 2$ and $d = 2$ ($\gamma_E \approx 0.577$).

Another observable of interest is the averaged avalanche duration at fixed size. In mean field, it is given by

$$\langle T \rangle_S / \tau_m = \sqrt{\pi S / S_m}, \tag{6}$$

which is consistent with the general expected scaling $\langle \tilde{T} \rangle_S \sim S^{1/\gamma}$, with $\gamma = \gamma^{MF}$. Remarkably, within mean field, Eq. (6) holds for any value of the ratio S/S_m.

Let us now consider the average temporal avalanche shape at fixed size, $\langle \dot{u}(t) \rangle_S$, which takes the form

$$\langle \dot{u}(t) \rangle_S = \frac{S}{\tau_m}\left(\frac{S}{S_m}\right)^{-1/\gamma} f\left(\frac{t}{\tau_m}\left(\frac{S_m}{S}\right)^{1/\gamma}\right), \tag{7}$$

where $f(t)$ is a universal scaling function, and $\int_0^\infty dt f(t) = 1$. In mean field, $f(t)$ is independent of S/S_m [24] and reads

$$f_{MF}(t) = 2te^{-t^2}. \tag{8}$$

Beyond MF, the function $f(t)$ has been obtained to $\mathcal{O}(\varepsilon)$ for SR elasticity. Here, we use the convenient form

$$f(t) \approx 2te^{-Ct^\delta} B \exp\left[-\frac{\epsilon}{9}\left(\frac{\delta f(t)}{f_{MF}(t)} - t^2 \ln(2t)\right)\right], \tag{9}$$

where the function $\delta f(t)$ is displayed in Eq. (34) of Ref. [23] and B is chosen such that $\int_0^\infty dt f(t) = 1$, an approximation exact to $\mathcal{O}(\varepsilon)$. Equation (9) has asymptotic behaviors

$$f(t) \simeq_{t \to 0} 2At^{\gamma-1}, \tag{10}$$

$$f(t) \simeq_{t \to \infty} 2A' t^\beta e^{-Ct^\delta}, \tag{11}$$

with $A = 1 + (\epsilon/9)(1 - \gamma_E)$, $A' = 1 + (\epsilon/36)(5 - 3\gamma_E - \ln 4)$, $\beta = 1 - \epsilon/18$, $C = 1 + (\epsilon/9)\ln 2$, and $\delta = 2 + \epsilon/9$.

To compare these theoretical predictions to our experimental results, we first need to make use of dimensionless units, thus rescaling sizes and durations by S_m and τ_m, respectively. The parameter S_m is analytically defined by Eq. (1); we tested that it leads to a consistent comparison of the measured size distribution $P(S)$ with the theory, see the Supplemental Material [27]. In particular, we verified that the cutoff occurs at $4S_m$, as predicted. On the other hand, τ_m can only be inferred using (i) the expression of Eqs. (2) and (6) and (ii) the data of the average shape $\langle \dot{u}(t) \rangle_S$. In absence of ECs, the estimation of τ_m is made by matching both kinds of data with the analytical expressions, giving a
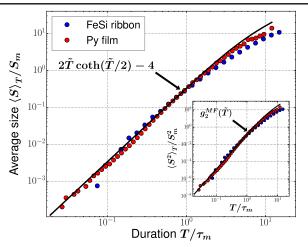
FIG. 1.   Normalized average size $\langle S \rangle_T / S_m$ of Barkhausen avalanches in the FeSi ribbon (blue dots) and the Py thin film (red dots) as a function of the normalized duration $\tilde{T} = T/\tau_m$. The continuous line is the theoretical prediction g_1^{MF} of Eq. (4). For the ribbon, the deviation at large durations is more evident due to effect of the eddy currents. The inset shows the second moment $\langle S^2 \rangle_T / S_m^2$ compared to the prediction g_2^{MF} of Eq. (4).
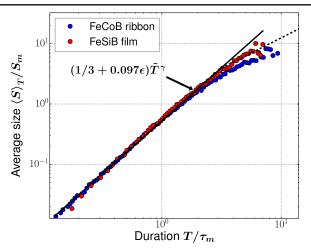

FIG. 2.   Normalized average size $\langle S \rangle_T / S_m$ of avalanches in the FeCoB ribbon (blue dots) and the FeSiB thin film (red dots) as a function of T/τ_m. The continuous line is the theoretical prediction of Eq. (5), with $\epsilon = 2$, so that $\langle S \rangle_T / S_m \sim 0.527 (T/\tau_m)^\gamma$, with $\gamma \sim 1.76$. The ribbon shows a larger deviation due to eddy currents. A comparison with the expected linear behavior at large $\tilde{T}$ is indicated by the dashed line. Remarkably, this deviation occurs at sizes larger than the size cutoff $4S_m$, i.e., for $\langle S \rangle_T / S_m > 4$.

consistent and robust estimation of the parameter [28]. In presence of ECs, we use the procedure (i) to estimate τ_m.

We analyzed the avalanche statistics in different classes of materials. Two of them are thin films with negligible eddy-current effects: a LR polycrystalline $Ni_{81}Fe_{19}$ Permalloy (Py) with a thickness of 200 nm ($\tau_m = 39\ \mu s$) and a SR amorphous $Fe_{75}Si_{15}B_{10}$ (FeSiB) alloy with a thickness of 1000 nm ($\tau_m = 38\ \mu s$) [30,31]. The other two samples are ribbons with a thickness of about 20 μm, where eddy-current retarding effects are well known: a LR polycrystalline FeSi alloy with Si = 7.8% ($\tau_m = 2$ ms), and a SR amorphous $Fe_{64}Co_{21}B_{15}$ (FeCoB) alloy, measured under a small tensile stress of 2 MPa ($\tau_m = 0.5$ ms) [5,17]. All samples have a space dimension $D = 2 + 1$; the two LR materials show MF exponents, while the other ones have NF exponents, with $\epsilon = 2$. Further details on the samples and the experiments are given in the Supplemental Material [27].

Figures 1 and 2 report the average size as a function of avalanche duration for LR and SR samples, respectively, compared to the theoretical prediction of Eqs. (4) and (5). In the absence of eddy currents, the correspondence is almost perfect, except for the highest (S, T) values. For LR samples (Fig. 1), the mean-field prediction (4) crosses over from $\sim \tilde{T}^2$ to $\sim \tilde{T}$ at large avalanche sizes, a trend which seems to agree with our data. It is often argued that a linear dependence can also arise from the superposition of a multiplicity of active DWs. Indeed some of the largest avalanches are a superposition of smaller avalanches occurring in different parts of the sample, triggered by the relatively large change of the magnetization [32]. Furthermore, the retarding effect of eddy currents makes

large avalanches (say, for $S > S_m$) even longer, so that the average size further deviates from the theoretical prediction, especially in samples with more ECs, as seen from Fig. 1. Note that the agreement with the MF predictions is also quite good at the level of fluctuations (i.e., the second moment $\langle S^2 \rangle_T$ in the inset of Fig. 1). For the SR samples in Fig. 2, we plot the prediction for small $\tilde{T}$, in good agreement with the data up to the size cutoff $4S_m$, i.e., $\langle S \rangle_T / S_m \sim 4$. At large $\tilde{T}$ we expect a similar bending to a
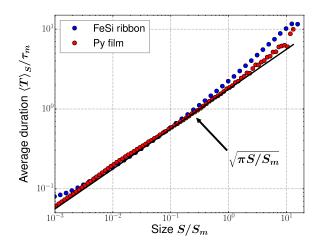

FIG. 3.   Normalized average duration $\langle T \rangle_S / \tau_m$ of avalanches in the FeSi ribbon (blue dots) and the Py thin film (red dots) as a function of the normalized size S/S_m. The continuous line is the theoretical prediction of Eq. (6).
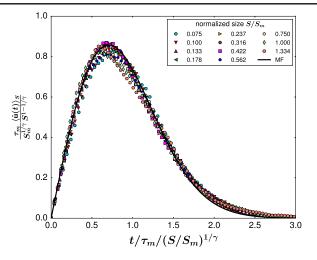
FIG. 4. Scaling collapse of the average shapes at fixed avalanche sizes $\langle \mathsf{u}(t) \rangle_S$, according to Eq. (7), in the Py thin film. The continuous line is the mean-field universal scaling function in Eq. (8).

linear behavior, although there are presently no detailed predictions for the crossover.

The mean avalanche duration at fixed size, $\langle T \rangle_S$, is shown in Fig. 3 for LR samples. For the film, it shows an almost perfect agreement with the MF prediction of Eq. (6), indicating that ECs are indeed negligible, while the effect of ECs is clearly visible in the ribbon.

Collapsing the experimental data of the average shapes at fixed size $\langle \dot{\mathsf{u}}(t) \rangle_S$ gives a powerful alternative way to estimate the exponent γ, as reported in Figs. 4 and 5. Here we obtain the same exponents as from the average size
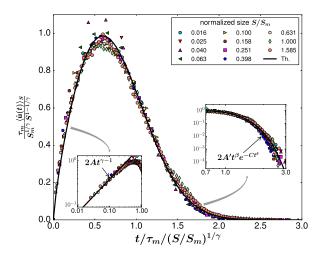

FIG. 5. Scaling collapse of the average shape at fixed avalanche sizes $\langle \dot{\mathsf{u}}(t) \rangle_S$, according to Eq. (7), in the FeSiB thin film. The continuous line is the prediction for the universal SR scaling function of Eq. (9). The insets show comparisons of the tails of the data with the predicted asymptotic behaviors of Eqs. (10) and (11), setting $\epsilon = 2$, with $A = 1.094$, $A' = 1.1$, $\beta = 0.89$, $C = 1.15$, and $\delta = 2.22$.

measurements $\langle S \rangle_T$; i.e., $\gamma = 2$ and $\gamma = 1.76$ for LR and SR, respectively. The collapsed average shapes correspond remarkably well to the theoretical predictions of Eqs. (8) and (9), including the behavior in the tails (shown in the SR case in the insets of Fig. 5). In the Supplemental Material [27], we further verify that neither the collapse nor the quantitative fit can be achieved using the MF prediction.

Finally, it is well known that relaxation of eddy currents introduces a slow time scale into the dynamics, stretching avalanches in time [24]. In Fig. 6, we have obtained an approximate collapse for the SR case in presence of eddy currents, using the theoretical value of $\gamma = 1.76$. It is manifest that the resulting curve is different from the one predicted in absence of retardation effects. Hence, this is another unambiguous method to detect the presence of ECs, similarly to the leftward asymmetry of the temporal avalanche shapes at fixed durations [25]. To go further and obtain predictions for the average shape in presence of ECs is difficult, as the shape strongly depends on the detailed parameters of the eddy currents. A step in that direction was obtained within MF in Ref. [24] for a particular model of retardation. Detailed comparison with experiments involve nonuniversal scales, and is left for a future publication.

In conclusion, we have shown how the data from Barkhausen noise experiments can be analyzed and compared to the most precise recent theoretical predictions. This provides quantitative and fundamental tests of the theory of avalanches beyond scaling exponents. The prediction of universality will also lead to a better characterization of magnetic systems, allowing us to measure its dimensionality and, via the deviations from the theory, effects of multiple avalanches or eddy currents.
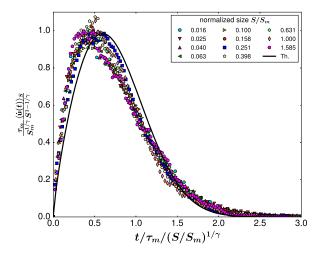

FIG. 6. Scaling collapse of the average shape at fixed avalanche sizes $\langle \dot{\mathsf{u}}(t) \rangle_S$ in the FeCoB ribbon using the theoretical values of γ and τ_m, as in Fig. 2. The collapse deviates from the universal functions predicted for SR systems (continuous black line) in the absence of eddy currents.

---

[1] H. Barkhausen, Zwei mit Hilfe der neuen Verstärker entdeckte Erscheinugen, Phys. Z. **20**, 401 (1919).

[2] J. S. Urbach, R. C. Madison, and J. T. Markert, Interface Depinning, Self-Organized Criticality, and the Barkhausen Effect, Phys. Rev. Lett. **75**, 276 (1995).

[3] D. H. Kim, S.-B. Choe, and S.-C. Shin, Direct Observation of Barkhausen Avalanche in Co Thin Films, Phys. Rev. Lett. **90**, 087203 (2003).

[4] V. Repain, M. Bauer, J.-P. Jamet, J. Ferré, A. Mougin, C. Chappert, and H. Bernas, Creep motion of a magnetic wall: Avalanche size divergence, Europhys. Lett. **68**, 460 (2004).

[5] G. Durin and S. Zapperi, in *The Science of Hysteresis: Physical Modeling, Micromagnetics, and Magnetization Dynamics* (Academic Press, Amsterdam, 2006), Vol. 2, Chap. 3, pp. 181–267.

[6] S. Papanikolaou, F. Bohn, R. L. Sommer, G. Durin, S. Zapperi, and J. P. Sethna, Universality beyond power laws and the average avalanche shape, Nat. Phys. **7**, 316 (2011).

[7] P. Le Doussal, K. J. Wiese, S. Moulinet, and E. Rolley, Height fluctuations of a contact line: A direct measurement of the renormalized disorder correlator, Europhys. Lett. **87**, 56001 (2009).

[8] S. Moulinet, C. Guthmann, and E. Rolley, Roughness and dynamics of a contact line of a viscous fluid on a disordered substrate, Eur. Phys. J. E **8**, 437 (2002).

[9] D. Bonamy, S. Santucci, and L. Ponson, Crackling Dynamics in Material Failure as the Signature of a Self-Organized Dynamic Phase Transition, Phys. Rev. Lett. **101**, 045501 (2008).

[10] L. Laurson, X. Illa, S. Santucci, K. T. Tallakstad, K. J. Måløy, and M. J. Alava, Evolution of the average avalanche shape with the universality class, Nat. Commun. **4**, 2927 (2013).

[11] N. Shapira, Y. Lamhot, O. Shpielberg, Y. Kafri, B. J. Ramshaw, D. A. Bonn, R. Liang, W. N. Hardy, and O. M. Auslaender, Disorder-induced power-law response of a superconducting vortex on a plane, Phys. Rev. B **92**, 100501(R) (2015).

[12] B. Alessandro, C. Beatrice, G. Bertotti, and A. Montorsi, Domain-wall dynamics and Barkhausen effect in metallic ferromagnetic materials. I. Theory, J. Appl. Phys. **68**, 2901 (1990).

[13] B. Alessandro, C. Beatrice, G. Bertotti, and A. Montorsi, Domain-wall dynamics and Barkhausen effect in metallic ferromagnetic materials. II. Experiments, J. Appl. Phys. **68**, 2908 (1990).

[14] F. Colaiori, Exactly solvable model of avalanches dynamics for Barkhausen crackling noise, Adv. Phys. **57**, 287 (2008).

[15] D. S. Fisher, Collective transport in random media: From superconductors to earthquakes, Phys. Rep. **301**, 113 (1998).

[16] S. Zapperi, P. Cizeau, G. Durin, and H. E. Stanley, Dynamics of a ferromagnetic domain wall: Avalanches, depinning transition, and the Barkhausen effect, Phys. Rev. B **58**, 6353 (1998).

[17] G. Durin and S. Zapperi, Scaling Exponents for Barkhausen Avalanches in Polycrystalline and Amorphous Ferromagnets, Phys. Rev. Lett. **84**, 4705 (2000).

[18] P. Le Doussal and K. J. Wiese, Size distributions of shocks and static avalanches from the functional renormalization group, Phys. Rev. E **79**, 051106 (2009).

[19] A. Rosso, P. Le Doussal, and K. J. Wiese, Avalanche-size distribution at the depinning transition: A numerical test of the theory, Phys. Rev. B **80**, 144204 (2009).

[20] P. Le Doussal and K. J. Wiese, Distribution of velocities in an avalanche, Europhys. Lett. **97**, 46004 (2012).

[21] A. Dobrinevski, P. Le Doussal, and K. J. Wiese, Nonstationary dynamics of the Alessandro-Beatrice-Bertotti-Montorsi model, Phys. Rev. E **85**, 031105 (2012).

[22] P. Le Doussal and K. J. Wiese, Avalanche dynamics of elastic interfaces, Phys. Rev. E **88**, 022106 (2013).

[23] A. Dobrinevski, P. Le Doussal, and K. J. Wiese, Avalanche shape and exponents beyond mean-field theory, Europhys. Lett. **108**, 66002 (2014).

[24] A. Dobrinevski, P. Le Doussal, and K. J. Wiese, Statistics of avalanches with relaxation and Barkhausen noise: A solvable model, Phys. Rev. E **88**, 032106 (2013).

[25] S. Zapperi, C. Castellano, F. Colaiori, and G. Durin, Signature of effective mass in crackling-noise asymmetry, Nat. Phys. **1**, 46 (2005).

[26] L. Laurson, X. Illa, S. Santucci, K. T. Tallakstad, K. J. Måløy, and M. J. Alava, Evolution of the average avalanche shape with the universality class, Nat. Commun. **4**, 2927 (2013).

[27] See Supplemental Material at http://link.aps.org/supplemental/10.1103/PhysRevLett.117.087201 for details on the samples and the experiments, the two universality classes, and on various tests showing that SR data cannot be described by MF predictions.

[28] Its actual value depends on the threshold that defines the start of the avalanche [5]; however, the latter can safely be set within a range where the critical exponents' estimation is robust, as explained in [29].

[29] L. Laurson, X. Illa, and M. J. Alava, The effect of thresholding on temporal avalanche statistics, J. Stat. Mech. (2009) P01019.

[30] F. Bohn, M. A. Corrêa, M. Carara, S. Papanikolaou, G. Durin, and R. L. Sommer, Statistical properties of Barkhausen noise in amorphous ferromagnetic films, Phys. Rev. E **90**, 032821 (2014).

[31] F. Bohn, M. A. Corrêa, A. Da Cas Viegas, S. Papanikolaou, G. Durin, and R. L. Sommer, Universal properties of magnetization dynamics in polycrystalline ferromagnetic films, Phys. Rev. E **88**, 032811 (2013).

[32] R. A. White and K. A. Dahmen, Driving Rate Effects on Crackling Noise, Phys. Rev. Lett. **91**, 085702 (2003).